Reaction of 2,3-Dichloro-5,6-dicyano-*p*-benzoquinone with 1,10-Phenanthroline and the Crystal Structure of Its Reaction Product

Masashi TANAKA,* Munekata OYAMA, Jun-ichi MIZOGUCHI,† and Setsuo KASHINO†
Department of Chemistry, Faculty of General Education, Nagoya University, Chikusa-ku, Nagoya 464-01
†Department of Chemistry, Faculty of Science, Okayama University, Tsushima, Okayama 700
(Received December 28, 1992)

2,3-Dichloro-5,6-dicyano-*p*-benzoquinone reacted with 1,10-phenanthroline to give 1,10-phenanthrolinium 4,5-dichloro-2-cyano-3,6-dioxo-1,4-cyclohexadien-1-olate. The reaction in acetonitrile solution was observed by the stopped flow technique and the UV-visible absorption spectra measurement. The crystal structure of its reaction product was determined by the X-ray diffraction study. The crystal was monoclinic, space group $P2_1$ with $a=12.323(4)$, $b=4.897(2)$, $c=13.677(3)$ Å, $\beta=96.51(3)°$, $V=820.0(8)$ Å^3, $Z=2$, and final $R=0.041$ for 1280 reflections larger than $3\sigma(I_o)$. The planar cations and anions stack along the b axis, respectively, to form the segregated columns.

p-Benzoquinone derivatives play an important role in bioorganic redox reactions and the modification reaction of *p*-benzoquinones were paid much attention in the synthetic chemistry.[1—3] Recently, the reactions of *p*-benzoquinones as electron acceptors with aromatic amines as donors were reported to proceed via the intermediate state with the character of a charge-transfer (CT) complex between the donor and acceptor molecules.[4,5] However, very few reports on the reaction of heterocyclic aromatic compounds with *p*-benzoquinones have been reported. In this paper, we report the reactions of 2,3-dichloro-5,6-dicyano-*p*-benzoquinone (DDQ) with 1,10-phenanthroline (phen) and the crystal structure of the reaction product, 1,10-phenanthrolinium 4,5-dichloro-2-cyano-3, 6-dioxo-1,4-cyclohexadien-1-olate (phenH DDQH), determined by the X-ray diffraction study. Furthermore, we report the reaction mechanism obtained by means of the stopped flow technique and the UV-visible absorption spectral change measurement with time.

Experimental

The Reaction of DDQ with Phen. 2,3-Dichloro-*p*-benzoquinone and 1,10-phenanthroline were commercially obtained and used without purification. UV-visible spectra were measured with a Hitachi 330 spectrophotometer. The stopped-flow measurement were made by using Unisoku stopped-flow rapid scan spectrophotometer RSP-601.

Crystal Structure Analysis of the Reaction Product (PhenH DDQH). Red-brown crystals of phenH DDQH elongated along the b axis and bounded by {001} and {100} planes were grown by slow evaporation of an acetonitrile solution of an equimolar mixture of DDQ and phen at room temperature. A crystal with the dimensions 0.63×0.10×0.08 mm was mounted on a glass fiber. Diffraction measurements were made on a Rigaku AFC-5R diffractometer with graphite monochromatized Mo Kα radiation ($\lambda=0.71073$ Å, 40 kV, 200 mA). Cell constants were determined from a least-square refinement using 2θ values of 25 reflections in the 2θ range of 19 to 22°.

The crystal data: $[C_{12}H_9N_2]^+[C_7NO_3Cl_2]^-$, $M_r=398.20$,

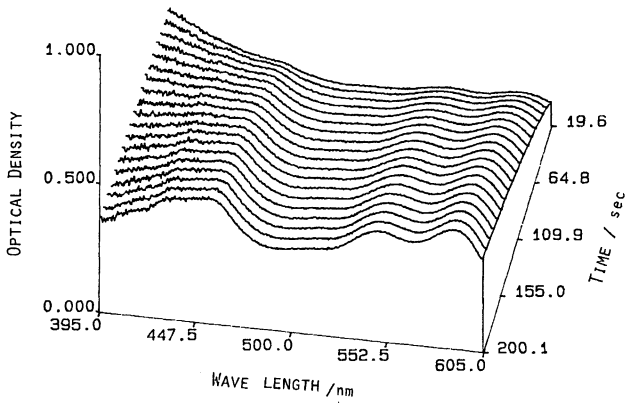

Fig. 1. Spectral change measured by the stopped flow method of the reaction of DDQ (1.0×10^{-2} M, 1 M=1 mol dm^{-3}) with phen (1.0×10^{-2} M) in acetonitrile solution at 25 °C.

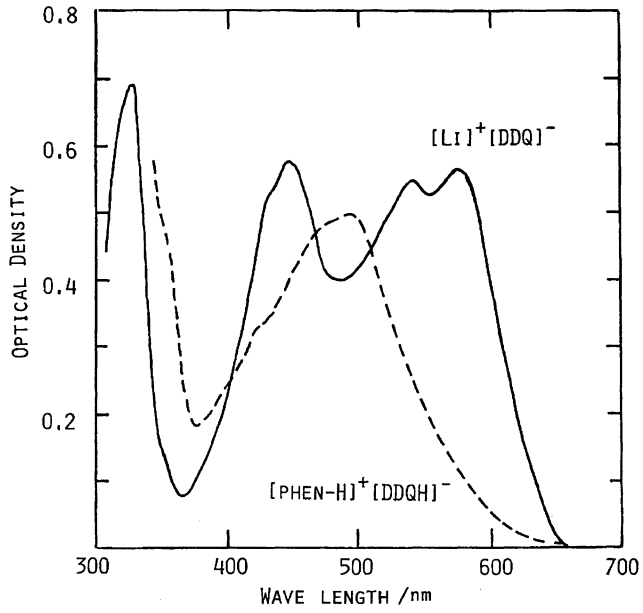

Fig. 2. Absorption spectra of LiDDQ (1.36×10^{-4} M) and the reaction product phenH DDQH (4×10^{-2} M) of DDQ with phen in acetonitrile solution.

monoclinic, $P2_1$. a=12.323(4), b=4.897(2), c=13.677(3) Å, β=96.51(3)°, V=820.0(8) Å^3, Z=2. D_m=1.62 (by flotation in trichloroethane and tribromoethane mixture), D_x=1.612 kg dm^{-3}. μ(Mo$K\alpha$)=0.42 mm^{-1}. F(000)=404.

The intensity data were collected at 298 K using the ω–2θ scan method to a maximum 2θ of 55° [scan width (1.63+0.30 tanθ)° in 2θ, scan speed 6 ° min^{-1} in ω]. Of 2200 reflections (ranging h=0 to 16, k=0 to 6, l=−18 to 18) 2108 were unique (R_{int}=0.013). The fluctuations of the intensities of three standard reflections, which were measured after every 97 reflections, were within 0.9%. An absorption correction based on azimuthal scans of three reflections was applied, the transmission factors ranging from 0.98 to 1.00. The data were corrected for Lorentz and polarization effects.

The structure was solved by direct method (MITHRIL[6]). The non-H atoms were refined anisotropically by full-matrix least-square method. The H atoms were found in a difference Fourier map, and refined isotropically. The final cycle of least-squares was based on 1280 reflections larger than 3σ (I_o) and 279 variable parameters. $\Sigma w(|F_o|-|F_c|)^2$ was minimized with $w=1/\sigma^2(F_o)$. Final R=0.041, wR=0.027, and S=1.31. $(\Delta/\sigma)_{max}$ was 0.3. The maximum and minimum $\Delta\rho$ in the final difference Fourier map were 0.31 and −0.27

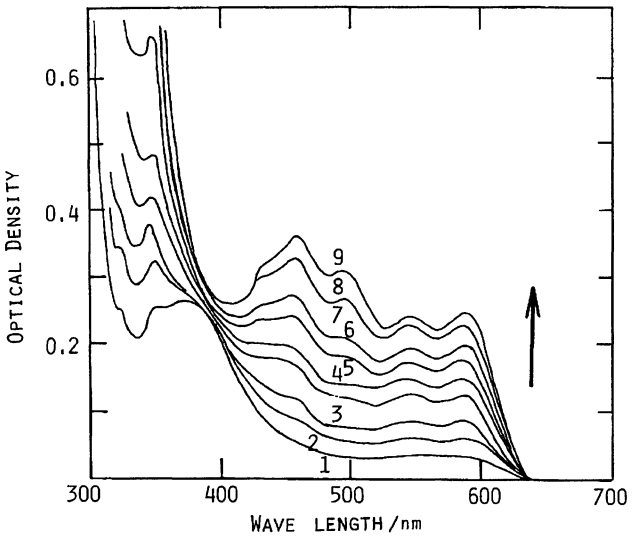

Fig. 3. Spectral change of the reaction of DDQ (1.0×10^{-2} M) with phen (1.0×10^{-2} M) in acetonitrile solution at 25 °C after (1) 0.3 h; (2) 1 h; (3) 2 h; (4) 3 h; (5) 4 h; (6) 20 h; (7) 40 h; (8) 50 h; (9) 95 h.

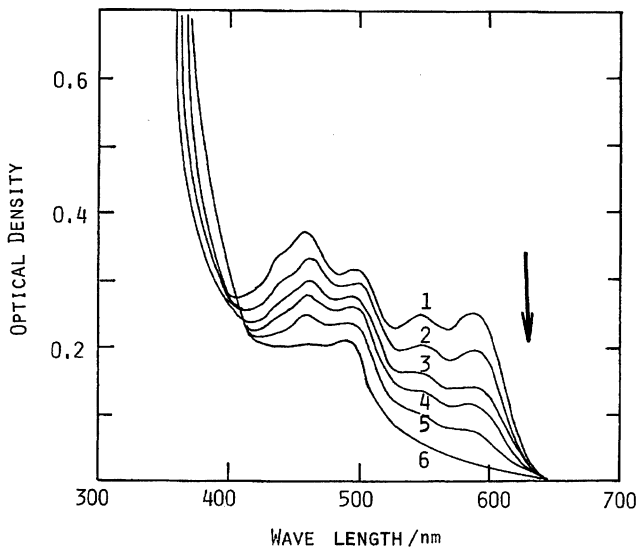

Fig. 4. Spectral change of the reaction of DDQ (1.0×10^{-2} M) with phen (1.0×10^{-2} M) in acetonitrile solution at 25 °C after (1) 95 h; (2) 144 h; (3) 187 h; (4) 192 h; (5) 264 h; (6) 408 h.

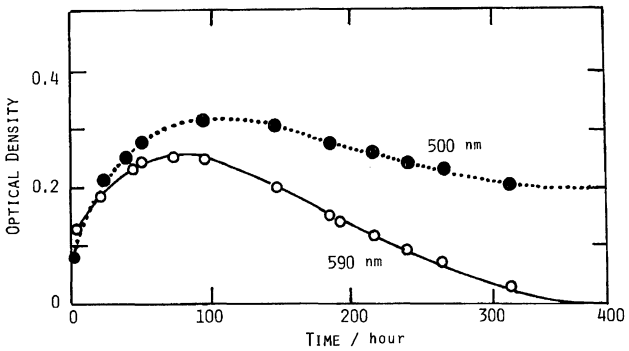

Fig. 5. Variation of the absorption intensity at 500 and 590 nm of the reaction of DDQ (1.0×10^{-2} M) with phen (1.0×10^{-2} M) in acetonitrile solution at 25 °C.

Table 1. Fractional Atomic Coordinates and Equivalent Thermal Parameters B_{eq} with Their esd's in Parentheses $B_{eq}=(8\pi^2/3)\sum_i\sum_j U_{ij}[a_i]^*[a_j]^* \boldsymbol{a}_i\cdot\boldsymbol{a}_j$

Atom	x	y	z	B_{eq}/Å^2
Cl(1)	0.1167(1)	1.2108(4)	0.5199(1)	4.14(7)
Cl(2)	0.3743(1)	1.2896(4)	0.51818(9)	3.88(7)
O(1)	0.0660(2)	0.796(1)	0.6559(2)	3.9(2)
O(2)	0.4944(3)	0.9268(9)	0.6578(2)	3.8(2)
O(3)	0.4245(3)	0.5400(9)	0.7758(2)	3.9(2)
N(1)	0.6119(3)	0.972(1)	0.9115(3)	3.4(2)
N(2)	0.6519(3)	0.592(1)	0.7744(3)	2.9(2)
N(3)	0.1592(3)	0.296(1)	0.8276(3)	4.6(3)
C(1)	0.5973(4)	1.166(1)	0.9775(4)	4.0(3)
C(2)	0.6791(5)	1.329(1)	1.0234(4)	3.6(3)
C(3)	0.7825(4)	1.294(2)	1.0015(3)	3.1(3)
C(4)	0.9114(4)	1.044(1)	0.9055(4)	3.0(3)
C(5)	0.9291(4)	0.853(1)	0.8403(4)	3.3(3)
C(6)	0.8537(4)	0.491(1)	0.7239(4)	3.1(3)
C(7)	0.7662(5)	0.346(1)	0.6805(4)	3.1(3)
C(8)	0.6648(5)	0.398(1)	0.7077(4)	3.2(3)
C(9)	0.7170(4)	0.944(1)	0.8911(3)	2.4(2)
C(10)	0.8051(4)	1.098(1)	0.9335(3)	2.6(2)
C(11)	0.8412(3)	0.693(1)	0.7934(3)	2.4(2)
C(12)	0.7361(3)	0.737(1)	0.8195(3)	2.4(2)
C(13)	0.1652(4)	0.816(1)	0.6599(3)	2.8(2)
C(14)	0.2116(4)	1.026(1)	0.5937(3)	2.7(2)
C(15)	0.3177(4)	1.059(1)	0.5934(3)	2.5(2)
C(16)	0.3976(4)	0.897(1)	0.6578(3)	2.5(2)
C(17)	0.3546(4)	0.680(1)	0.7248(3)	2.7(2)
C(18)	0.2421(4)	0.655(1)	0.7218(3)	2.5(2)
C(19)	0.1965(4)	0.459(1)	0.7805(4)	3.2(3)

eÅ^{-3}.

The atomic scattering factors were taken from International Table for X-Ray Crystallography.[7] Calculations were performed by using the TEXAN[8] at the X-Ray Laboratory of Okayama University.

Results and Discussion

The Spectral Change in the Reaction of DDQ with Phen. A sample solution containing DDQ and phen (1.00×10^{-2} mol dm^{-3} for each of the reactants) were prepared freshly and the reaction temperature was kept at 25 °C. The reaction of DDQ with phen was carried out in acetonitrile solution. Figure 1 shows the spectral change measured by the stopped-flow technique. At the initial stage, the absorption peaks were observed at 590, 550, and 460 nm and these peaks may be assigned to the absorption bands ($\pi\rightarrow\pi^*$) of DDQ anion radical shown in Fig. 2.[9] Figure 3 represents the spectral change during the reaction between 20 min and 95 h. All absorption spectral intensities increased over all observed wavelength range and no isosbestic point was observed. The $n\rightarrow\pi^*$ peaks[10] ($\lambda_{max}=370$ nm and $\varepsilon_{max}=800$ l mol^{-1} cm^{-1}) of DDQ molecule remained unchanged at 20 min. As the reaction proceeds, the $n\rightarrow\pi^*$ at 370 nm was covered by the stronger absorption band at 350 nm, which is assigned to the $\pi\rightarrow\pi^*$ band of DDQ anion radical.[9] Furthermore, a new peak appeared at 500 nm. This band could be assigned to the reaction product of DDQ and phen, as is shown in Fig. 2. Figure 4 shows the spectral change with time after 95 h. The absorption intensities of the reaction solution decreased with time in the 300—700 nm re-

Table 2. Bond Lengths (l/Å) and Angles (ϕ/°)

Cl(1)–C(14)	1.713(5)	C(5)–C(11)	1.428(7)
Cl(2)–C(15)	1.726(5)	C(6)–C(7)	1.369(7)
O(1)–C(13)	1.222(5)	C(6)–C(11)	1.393(7)
O(2)–C(16)	1.201(5)	C(7)–C(8)	1.368(7)
O(3)–C(17)	1.249(6)	C(9)–C(10)	1.393(6)
N(1)–C(1)	1.335(7)	C(9)–C(12)	1.447(6)
N(1)–C(9)	1.362(5)	C(11)–C(12)	1.398(5)
N(2)–C(8)	1.337(7)	C(13)–C(14)	1.523(7)
N(2)–C(12)	1.349(6)	C(13)–C(18)	1.433(6)
N(3)–C(19)	1.157(7)	C(14)–C(15)	1.319(6)
C(1)–C(2)	1.381(8)	C(15)–C(16)	1.477(7)
C(2)–C(3)	1.352(7)	C(16)–C(17)	1.539(7)
C(3)–C(10)	1.389(7)	C(17)–C(18)	1.387(6)
C(4)–C(5)	1.327(7)	C(18)–C(19)	1.408(7)
C(4)–C(10)	1.430(6)		
C(1)–N(1)–C(9)	114.5(5)	C(9)–C(12)–C(11)	120.5(4)
C(8)–N(2)–C(12)	122.7(5)	O(1)–C(13)–C(14)	118.0(5)
N(1)–C(1)–C(2)	124.8(5)	O(1)–C(13)–C(18)	124.9(5)
C(1)–C(2)–C(3)	118.9(6)	C(14)–C(13)–C(18)	117.1(4)
C(2)–C(3)–C(10)	120.1(6)	Cl(1)–C(14)–C(13)	115.5(4)
C(5)–C(4)–C(10)	122.3(5)	Cl(1)–C(14)–C(15)	122.9(4)
C(4)–C(5)–C(11)	120.9(5)	C(13)–C(14)–C(15)	121.6(5)
C(7)–C(6)–C(11)	121.4(5)	Cl(2)–C(15)–C(14)	123.4(4)
C(6)–C(7)–C(8)	119.0(6)	Cl(2)–C(15)–C(16)	114.8(4)
N(2)–C(8)–C(7)	120.1(6)	C(14)–C(15)–C(16)	121.7(5)
N(1)–C(9)–C(10)	125.0(5)	O(2)–C(16)–C(15)	122.0(5)
N(1)–C(9)–C(12)	116.2(4)	O(2)–C(16)–C(17)	119.6(5)
C(10)–C(9)–C(12)	118.8(4)	C(15)–C(16)–C(17)	118.4(4)
C(3)–C(10)–C(4)	124.5(5)	O(3)–C(17)–C(16)	116.7(4)
C(3)–C(10)–C(9)	116.6(5)	O(3)–C(17)–C(18)	126.4(5)
C(4)–C(10)–C(9)	118.9(5)	C(16)–C(17)–C(18)	116.9(5)
C(5)–C(11)–C(6)	124.0(4)	C(13)–C(18)–C(17)	124.2(5)
C(5)–C(11)–C(12)	118.6(5)	C(13)–C(18)–C(19)	115.6(4)
C(6)–C(11)–C(12)	117.5(5)	C(17)–C(18)–C(19)	120.2(5)
N(2)–C(12)–C(9)	120.2(4)	N(3)–C(19)–C(18)	178.9(6)
N(2)–C(12)–C(11)	119.3(5)		

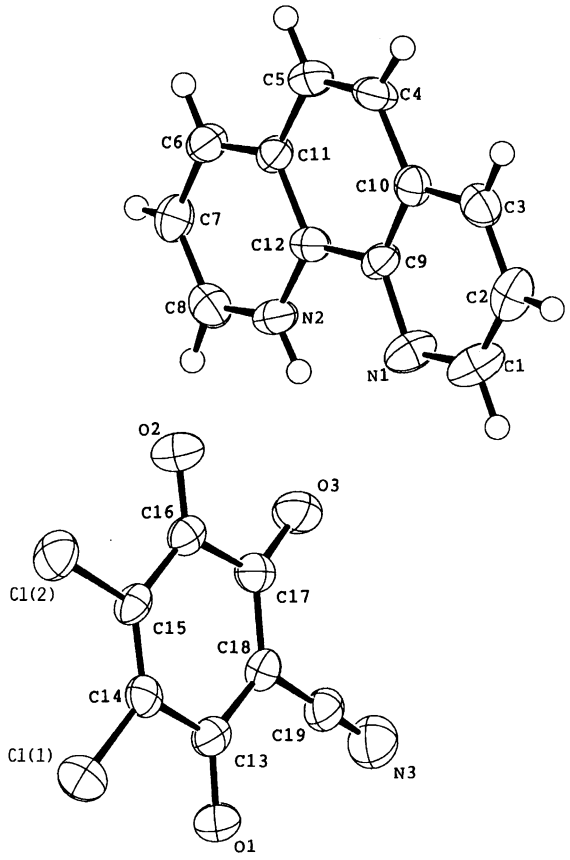

Fig. 6. The ORTEP drawing and atomic numbering of the cation (phenH) and the anion (DDQH). The thermal ellipsoids of 50% probability are used for non-H atoms. The H atoms are represented as spheres equivalent to $B=1.0$ Å^2.

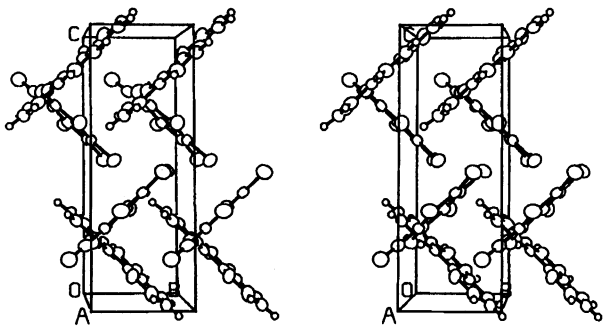

Fig. 7. The stereoscopic view of the crystal structure.

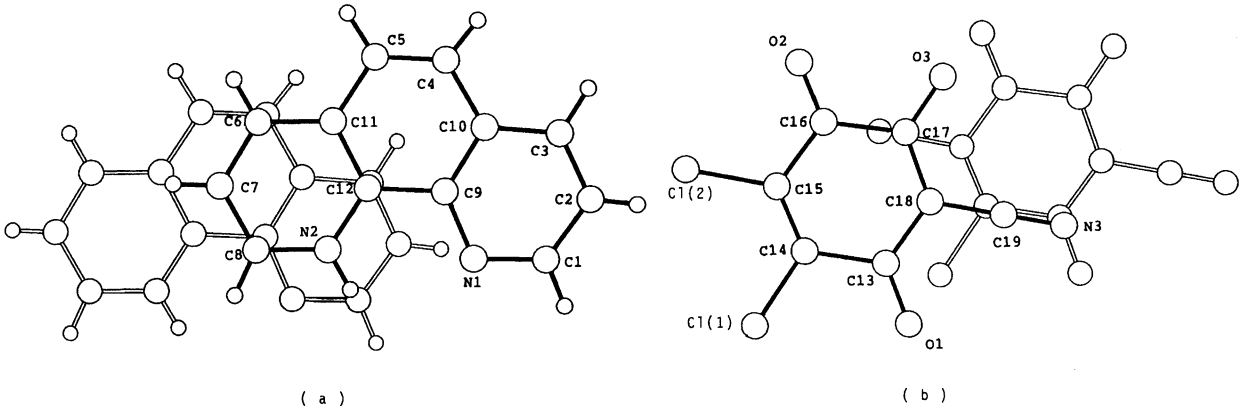

Fig. 8. The molecular overlapping. (a) the cation (phenH) and (b) the anion (DDQH).

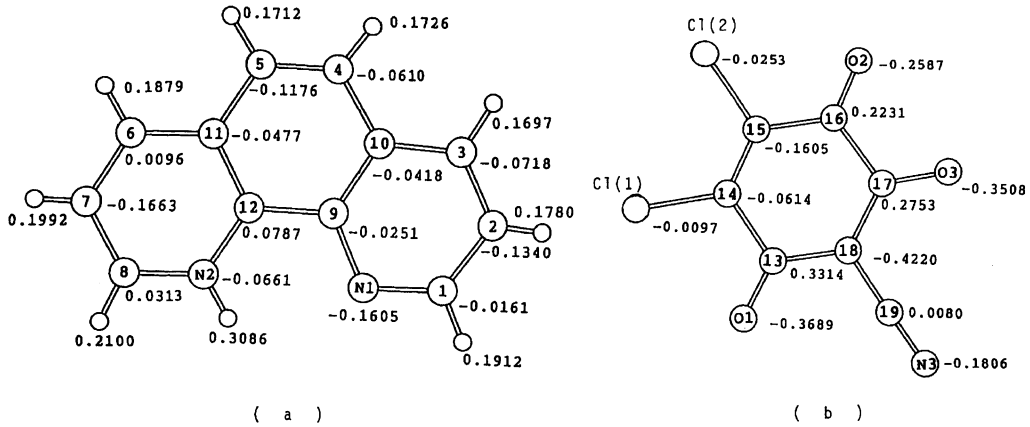

Fig. 9. The net atomic charges on atoms of (a) the cation (phenH) and (b) the anion (DDQH).

gion. Two peaks at 550 and 590 nm drastically disappeared and the remained absorption spectrum had the peaks at 500 nm which is similar to the absorption spectrum of DDQH as is shown in Fig. 2, because the protonation to phen takes place only minor changes in the spectral patterns of phen molecule[11] and the 500 nm absorption band has the spectral pattern similar to that of KDDQH.[9] Figure 5 depicts the absorption intensity change at 500 and 590 nm with time. That is, the above-mentioned reaction of DDQ with phen may proceed as follows (Chart 1):

The first reaction is the electron transfer reaction from phen to DDQ and the second is the protonation of the phen cation radical and the substitution of the cyano group of DDQ anion radical.

Crystal Structure of the Reaction Product (PhenH DDQH). Final atomic parameters are listed in Table 1.[12] On the contrary to the expectations observed in phenanthrene–DDQ[13] and benzo[*c*]cinnoline–DDQ[14] complexes, the structure is composed of the cation (phenH) and the anion (DDQH) as seen from the ORTEP drawing[15] in Fig. 6. The bond lengths and angles are listed in Table 2. Their values in the anion agree within the experimental errors with those previously found in potassium salt of DDQH.[16] The anion is planar within 0.05 Å. The large deviations from the plane are 0.032(5) Å at O(2) and −0.049(6) Å at N(3). In the cation, the inner angle at the protonated N(2), C(8)–N(2)–C(12), is significantly larger than the inner angle at the unprotonated N(1) and that found in 1,10-phenanthroline.[17] The cation is planar within 0.02 Å as a whole. However, the dihedral angle between the planes of the pyridinium and pyridine rings is 1.3-(2)°. The stereoscopic view of the crystal structure is shown in Fig. 7. The cations and the anions form the segregated columns along the *b* axis, respectively, with a dihedral angle of 86.93(5)° between the planes of the cation and the anion. The cation is linked to the anion

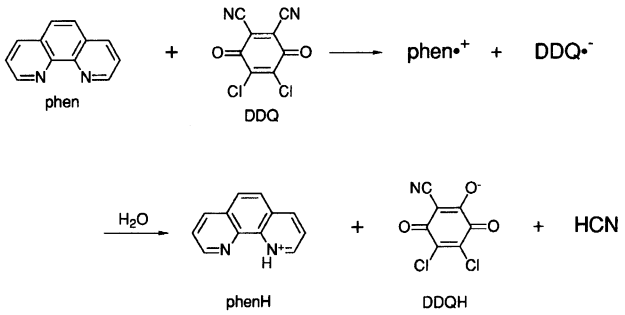

Chart 1.

through N–H···O hydrogen bond [N(2)···O(3) 2.816(5) Å, H(2N)···O(3) 2.04(4) Å, N(2)–H(2N)···O(3) 149°]. A short C–H···O interaction is found between the cation at x, y, z and the anion at x, $-1+y$, z [C(8)···O(2) 3.144(7) Å, H(8)···O(2) 2.28(6) Å, C(8)–H(8)···O(2) 153(5)°].

The molecular overlapping and the net atomic charges on atoms estimated by AM1 method, MOPAC Ver. 5. 02[18,19] are shown in Figs. 8 and 9, respectively. The pyridinium ring of one cation lies above another cation over the central phenylene and pyridine rings with an interplanar distance of 3.330(7) Å. It is noted that short interatomic contacts are found between the pairs of positively charged and negatively charged atoms: C(6)···C(4) 3.326(8), C(8)···C(9) 3.362(7), and C(12)···C(3) 3.302(7) Å. It is also found that H(2N) and H(7) with positive charges overlap on negatively charged C(1) and C(11), respectively. Interplanar distance between the overlapping anions is 3.340(7) Å. The atomic overlapping is not so prominent for the anions. However, short interatomic contacts are observed between positively charged and the negatively charged atoms: 3.442(5) Å for C(17)···C(12), 3.344(7) Å for C(19)···C(14), and 3.290(7) Å for C(13)···N(3).

References

1) S. Shiraishi, Y. Inoue, and K. Imamura, *Bull. Chem. Soc. Jpn.*, **64**, 2388 (1991).
2) T. Oshima and T. Nagai, *Bull. Chem. Soc. Jpn.*, **63**, 630 (1990).
3) A. M. Nour El-Din, A-F. E. Mourad, A. A. Hassen, and M. A. Gomaa, *Bull. Chem. Soc. Jpn.*, **64**, 1966 (1991).
4) T. Nogami, T. Yamaoka, K. Yoshihara, and S. Nagakura, *Bull. Chem. Soc. Jpn.*, **44**, 380 (1971).
5) Y. Osawa, N. Nishimura, and S. Yamamoto, *Bull. Chem. Soc. Jpn.*, **64**, 2648 (1991).
6) G. J. Gilmore, *J. Appl. Crystallogr.*, **17**, 42 (1984).
7) "International Tables for X-Ray Crystallography." Kynoch Press, Birmingham (Present distributor Kluwer Academic Publisher, Dordrecht) (1974), Vol. IV, pp. 22—98.
8) "TEXSAN. Single Crystal Structure Analysis Software. Version 5.0," Molecular Structure Corporation, The Woodlands, Texas (1989).
9) J. S. Miller, P. J. Krusic, D. A. Dixon, W. M. Reiff, J. H. Zhang, E. C. Anderson, and A. J. Epstein, *J. Am. Chem. Soc.*, **108**, 4459 (1986).
10) M. Tanaka, S. Murata, H. Takeuchi, and S. Matsuo, *Bull. Chem. Soc. Jpn.*, **65**, 2157 (1992).
11) M. Yamada, M. Kimura, M. Nishizawa, S. Kuroda, and I. Shimao, *Bull. Chem. Soc. Jpn.*, **64**, 1821 (1991).
12) Tables of anisotropic thermal parameters, atomic parameters of hydrogen atoms, bond lengths and angles involving hydrogen atoms, and structure factors have been deposited as Document No. 66017 at the Office of the Editor of Bull. Chem. Soc. Jpn.
13) F. H. Herbstein, M. Kapon, G. Rzonzew, and D. Rabinovich, *Acta Crystallogr., Sect. B*, **34**, 476 (1978).
14) J. Bernstein, H. Regev, and F. H. Herbstein, *Acta Crystallogr., Sect. B*, **33**, 1716 (1977).
15) C. K. Johnson, "ORTEP II, Report ORNL-5138," Oak Ridge National Laboratory, Tennessee (1976).
16) M. Konno, *Acta Crystallogr., Sect. C*, **40**, 236 (1984).
17) S. Nishigaki, H. Yoshida, and K. Nakatsu, *Acta Crystallogr., Sect. B*, **34**, 875 (1978).
18) J. J. P. Stewart, *QCPE Bull.*, **9**, 10 (1989).
19) T. Hirano, *JCPE Newsletter*, **1**, 10 (1989).